Remineralizing effect of a new strontium-doped bioactive glass and fluoride on demineralized enamel and dentine

Abstract

Objective: *To investigate the remineralizing effect of a strontium-doped bioactive glass (HX-BGC) and fluoride on demineralized enamel and dentine.*

Materials: *Sixty demineralized human tooth specimens were allocated to four groups. Group 1 received 5% HX-BGC, Group 2 received 5% HX-BGC and 1,450 ppm fluoride, Group 3 received 1,450 ppm fluoride, and Group 4 received deionized water as negative control. The specimens were subjected to pH cycling for 14 days. The surface morphology, lesion depths, crystal characteristics and collagen matrix degradation of the specimens were assessed by scanning electron microscopy (SEM), micro-computed tomography (mico-CT), X-ray diffraction (XRD), and spectrophotometry with a hydroxyproline (HYP) assay, respectively.*

Results: *SEM images showed the enamel surface was smooth with regularly arranged enamel rods in Groups 1 to 3. Granular grains were observed in both inter-tubular and intra-tubular dentine in Groups 1 to 3. The mean lesion depths in enamel were 80.8 μm, 50.6 μm, 72.7 μm and 130.7 μm in Groups 1 to 4, respectively ($p<0.001$), and those in dentine were 152.6 μm, 140.9 μm, 165.4 μm and 214.1 μm, respectively ($p<0.001$). The differences in mean mineral loss in enamel and in dentine between the four study groups follow the same pattern as that of the differences in lesion depth. XRD illustrated apatite formation in each group. There were no significant differences in the HYP concentrations among the four groups ($p=0.261$).*

Conclusion: *Combined use of HX-BGC and fluoride can reduce mineral loss and promote remineralization of demineralized enamel and dentine through the precipitation of newly formed apatite.*

Clinical significance: *Adjunctive use of HX-BGC may enhance the remineralization effect of fluoride in the management of early dental caries lesions.*

Key words*: bioactive glass, fluoride, remineralization, enamel, dentine, caries*

1. Introduction

Dental caries is a bacteria-mediated disease, which is an unfavourable outcome of a continuous process with many cycles of demineralization and remineralization in dental hard tissues, that can be viewed as an imbalance between biofilms and tooth minerals [1, 2]. Organic acids, as by-products of fermentation of carbohydrates, produced by cariogenic bacteria can diffuse into tooth subsurface and dissolve the minerals, causing demineralization. The dissolution of minerals on the tooth surface lead to exposure of dentine collagen and the low pH environment may activate the intrisinc matrix metalloproteinases (MMPs) which can cause collagen degradation [3]. Remineralization is a natural repair process which mainly relies on the deposition of calcium phosphate, primarily comes from saliva, to form a new layer on the lesion surface [1]. Contemporary approaches in caries management aim to arrest and prevent further development of caries [4]. Fluoride application is the usual method used to prevent demineralization and enhance remineralization [5]. However, the use of fluoride-containing products in treating and preventing dental caries can only reach a certain maximum effect. Therefore, additional use of other agents in the remineralization therapy is warranted, such as bioactive materials that can enhance remineralization in the presence of fluoride and act as a complement to fluoride [6, 7] .

Bioactive glass, a novel bioactive marterial, has been introduced and has a wide range of clinical applications in both medicine and dentistry [8]. One of the bioactive glasses, named 45S5 Bioglass, has been shown to have bone bonding ability and used for bone replacement in the middle ear to treat conductive hearing loss [9]. More recently, it is used for treatment of dentine hypersensitivity through blocking the dentinal tubules by its dissolution products precipitating and adhering to the surface of dentine, thereby relieving the pain [9, 10]. Bioactive glass is able to reduce dentine permeability and make the dentine surface more resistant to acids [11]. In addition, a review concluded that bioactive glass can form an apatite-like layer on the surface of enamel and dentine, and promote remineralization of carious lesions [12]. Strontium has recently attracted some interest in caries management due to its similarity with calcium [13] and cariostatic effect on dental caries [14]. Another study also reported that strontium can inhibit the expression of MMPs [15]. A new bioactive glass (HX-BGC, SiO_2-P_2O_5-Na_2O-SrO) with the addition of strontium was developed and studied [16]. A study showed that in the presence of HX-BGC, pH of the fluid was elevated and the growth of cariogenic bacteria was inhibited [16]. An earlier study found that strontium could act synergistically with fluoride [17].

Therefore, the present study aimed to investigate the remineralizing effect of a strontium-doped bioactive glass and fluoride on demineralized enamel and dentine. The null hypothesis was that the combined application of HX-BGC and fluoride would not enhance the remineralization of demineralized enamel and dentine.

2. Materials and methods

2.1 Preparation of specimens with artificial caries

This study was approved by the Institutional Review Board of the University of Hong Kong (UW 19-471). Fifteen extracted human molars were selected from the collection of extracted teeth of the Prince Philip Dental hospital, Hong Kong. These teeth were stored in a 0.5% thymol solution before use. The teeth were cut by a low-speed cutting machine (ISOMET 1000, Buehler, LakeBluff, IL, USA) under running deionized water to produce 60 specimens (4 specimens from each tooth) with a thickness of 2 mm in which there were both enamel and dentine in each specimen. The surface of the specimen was polished using micro-fine 4000 grid sandpaper and washed in deionized water. Then a stereomicroscope was used to examine the specimens to exclude those with cracks or defects.

The surfaces of each specimen were covered by an acid-resistant nail varnish, except for a window approximately 2 mm x 2 mm in size (Fig.1). The tooth specimens were then immersed in a demineralizing solution (2.2mM $CaCl_2$, 2.2mM KH_2PO_4, 50mM acetic acid, pH=4.4) at 37°C for 8 days to produce demineralized lesions in enamel and dentine. The lesions were scanned by X-ray micro-CT (SkyScan1172; SkyScan, Antwerp, Belgium) and the depths of lesions were measured by a NRecon reconstruction software (SkyScan, Antwerp, Belgium). The specimens were stored in deionized water at 4^{o}C and were subjected to different treatments the next day.

2.2 Experimental treatment

The HX-BGC powder used in this study was provided by Dencare (Chongqing) Oral Care Co. Ltd. In Group 1, the 5% (0.0526g/ml) HX-BGC suspension was prepared by adding 0.263g HX-BGC powder into 5ml deionized water. In Group 2, 0.0145g NaF powder and 0.263g HX-BGC powder were added into 5ml deionized water to form a suspension of HX-BGC with fluoride. In Group 3, the 1450 ppm fluoride solution was prepared by dissolving 0.0145g NaF powder in 5ml deionized water. The suspensions and solutions were made freshly

for one-day use and votexed for 20 seconds everytime before application. The four prepared specimens from the same tooth, with demineralized lesions in enamel and dentine, were randomly allocated into the four study groups (sample size = 15 in each group). In Group 1, the 5% HX-BGC suspension was applied onto the surface of the specimens. In Group 2, the specimens received an application of the 5% HX-BGC suspension with 1,450 ppm fluoride. In Group 3, the specimens were treated with 1,450 ppm fluoride solution. Group 4 was the negative control group in which deionized water was applied onto the surface of the specimens. All treatments were applied onto the surface of the tooth specimens with a micro-brush (Premium Plus International Ltd., Hong Kong) and waited for 2 minutes. Subsequently, the applied agents were removed by gently rinsing the specimen under a gentle jet of deionized water.

2.3 Assessment of the changes in the demineralized enamel and dentine

2.3.1 pH cycling

The pH cycling protocol used by Amaechi was employed to investigate the effect of the study agents on the demineralized enamel and dentine [18]. Before the pH cycling, the demineralized specimens were immersed in a remineralizing solution (1.5mM $CaCl_2$, 0.9mM NaH_2PO_4, 150mM KCl, pH=7.0) for 24 hours. Then they were pH cycled at room temperature. First, the specimen was taken out from the remineralizing solution and the corresponding study agent was applied onto the window of the specimen for 2 minutes according to its group allocation. Afterwards, the specimen was rinsed with deionized distilled water to remove the applied agent. This process, for all 60 specimens, took half an hour to complete, and then all the specimens were immersed in the demineralizing solution (1.5mM $CaCl_2$, 0.9mM KH_2PO_4, 50mM acetic acid, pH=4.5) for 8 hours. After the 8h demineralization, the specimens were rinsed with deionized distilled water and received application of the study agents as described above. Then, the specimens went through a 15h immersion in the remineralizing solution. All the specimens were pH-cycled through remineralization solution and demineralization solution every day for 14 days.

2.3.2 Morphology of enamel and dentine surface

Four pH-cycled specimens from each group were fixed in 2.5% glutaraldehyde for one night. They were placed in distilled water and cleaned ultrasonically three times, then followed by dehydration with a series of ethanol solutions (75%, 80%, 95%, 100% ethanol). The dehydrated specimens were critical-point dried as described in a previous study [19] in a

desiccator (Leica EM CPD300, Leica Microsystems, Gemany) and sputter-coated with carbon. The surface morphology of the specimens was observed under a scanning electron microscope (SEM, Hitachi S-4800FEG Scanning Electron Microscope, Hitachi Ltd., Tokyo, Japan) at high-vacuum mode after the above-mentioned procedure.

2.3.3 Lesion depth and mineral loss

Depths of the demineralized lesions in enamel and dentine were measured by micro-CT (SkyScan1172; SkyScan, Antwerp, Belgium) scanning. The voltage and current settings were 80kV and 100 μA, respectively. The image pixel size was set at 7.95 μm (maximum resolution) and the X-rays were cut-off by a 0.5 mm aluminium filter. Five specimens from each group were scanned and reconstructed by using the NRecon reconstruction software (SkyScan, Antwerp, Belgium). CT data analyzing software (SkyScan, Antwerp, Belgium) was used to view and analyze the reconstructed three-dimensional images. Ten reconstructed cross-sectional images from each specimen were randomly selected for the measurement of the lesion depth and mineral loss.

2.3.4 Crystal characteristics

Characteristics of the surface of the mineral crystals (2 specimens per group without any pretreatment) were assessed by an X-ray diffractometer (XRD, Rigaku SmartLab 9kW, Tokyo, Japan) equipped with a CuKα lamp ($\lambda = 1.54056$ Å). The parameters for collecting data were: 2θ range = 20º to 60º, step size = 0.02º and scan speed = 0.6 s/step. Collection of the diffraction data was performed twice so as to minimize error. A computer software, Jade 6 (MDI, California, United States), was used to analyze the XRD patterns. The diffraction patterns were drawn by Origin 81 (OriginLab, Northampton, Massachusetts, USA).

2.4 Dentine collagen degradation

To assess the effect of the study agents on collagen degradation, a modified amino acid hydroxyproline (HYP) assay was used [20]. In brief, enamel was removed from the specimens. Four specimens from each group, with dentine only and a standardized size of 2×5×5 mm, were pH cycled through the above-mentioned processes for 14 days. Afterwards, they were placed individually in separate tubes and 100 μL of 4N NaOH was added to each tube. Next, the specimens were autoclaved at 120℃ for half an hour, followed by allowing the specimens to return to room temperature for 20 min and addition of 100 μL of 4N HCl to each tube to neutralize the pH. Then, a buffered Chloramine-T solution (0.05M) was added into each tube,

mixed with the specimen, and oxidation at room temperature was allowed for 20 min. Afterwards, Ehrlich's solution (1M) was added and each tube was vortexed to ensure complete mixing. Finally, the tubes were placed in a water bath at 65℃ for 20 min. A HYP standard solution containing 2-200 μg HYP was prepared. The absorbance of the solutions was read at 550 nm by a microplate reader (SpectraMax® M2, California, USA).

2.5 Statistical analysis

Data obtained from the measurements were assessed by using Shapiro-Wilk normality test and one-way ANOVA was used to compare the lesion depths, mineral loss and concentration of HYP in the specimens of the four study groups. All analyses were conducted by using the statistical software IBM SPSS Statistics version 27. Statistical significance level was set at 0.05.

3. Results

Figures 2 and 3 show the transverse and longitudinal section surface morphology of the dentine lesions of the four groups. There were nearly no dentine collagen fibers exposed on the completely occluded surface of the specimens in Group 2 (HX-BGC+F) (Fig. 2c). Large granular structures in the inter-tubular areas were observed in the longitudinal section images in Group 1 (HX-BGC) and in Group 2 (Fig. 3a, 3b, and 3c), while the image of Group 2 also shows sparse spherical grains in the intra-tubular areas (Fig. 3d). Images of the specimen in Group 3 (F) show a relatively rough dentine surface with partial exposure of collagen fibers (Fig. 2e) and there was space in both the inter- and intra-tubular areas (Fig. 2f). The longitudinal section images show large inter-fibrillar distances and there were granular grains in the inter-tubular areas (Fig. 3e and f). In Group 4 (control), exposure of the reticular microstructure of collagen fibers on the dentine surface shows partial dentine demineralization (Fig. 2g). The collagen fibers were loose in both inter- and intra-tubular areas, as seen under higher magnification (Fig. 2h). Likewise, images of the longitudinal section show the sparsely distributed exposed collagen (Fig. 3g and 3h). No granular structure was observed in Group 4. Figure 4 shows the transverse section surface of the enamel lesions in the four groups. In Group 4, the surface was not smooth and the enamel rods were thinner (Fig. 4g), and obvious crevice and porosities among enamel rods appeared under higher magnification (Fig. 4h).

Figure 5 shows the micro-CT images of the enamel and dentine lesions after demineralization for 8 days in the four study groups. The precipitations in Group 2 and Group 3 had formed a new layer on the surface of dentine, while no obvious layer appeared on the enamel (Fig. 6). Mean depths and mineral loss of the lesions in enamel and dentine are shown in Table 1. The mean (± SD) dentine lesion depths of Groups 1, 2 and 3 were 152.60 ± 5.18 μm, 140.88 ± 12.82 μm and 165.36 ± 31.51 μm, respectively. The mean lesion depths of these three groups were significantly smaller ($p<0.001$) than that of Group 4 (control), which was 214.12 ± 11.08 μm . The mean (± SD) enamel lesion depth of Group 2 (HX-BGC+F) was 50.60 ± 10.65 μm, which was significantly smaller ($p<0.001$) than those of Groups 1 and 3, which were 80.84 ± 2.43 μm and 72.67 ± 12.73 μm, respectively. The mean enamel lesion depth of Group 4, at 130.66 ± 12.31 μm, was the largest ($p<0.001$). The mean mineral loss of dentine in Groups 1 to 3 were 1.64 ± 0.09 g/cm^3, 1.54 ± 0.11 g/cm^3 and 1.77 ± 0.08 g/cm^3, respectively, while Group 4 had the largest mineral loss which was 2.12 ± 0.08 g/cm^3 ($p<0.001$). Similarly, the mineral loss of enamel in Group 4 was 3.44 ± 0.07 g/cm^3, significantly ($p<0.001$) larger than that of Group 2, which was 2.94 ± 0.21 g/cm^3 (p=0.04).

Typical XRD patterns of the mineral crystals in the four groups are shown in Figure 7. The pattern of scattered X-ray in Group 4, which corresponded to (002), (210), (211) and (300) Bragg reflections, indicated that the precipitates deposited on the surface of enamel and dentine were similar to apatite. The (300) reflection in Group 1 was 31.68º (2θ) and the lower 2θ value compared with that of Group 4 (31.78º) shows strontium incorporation in the apatite crystals.

The mean HYP concentrations, reflecting the amount of degraded collagen, of Groups 1 to 4 were 346.25 ± 2.87 μg/mL, 344.25 ± 24.39 μg/mL, 364.75 ± 3.69 μg/mL and 345.50 ± 19.63 μg/mL, respectively. There were no statistically significant differences ($p=0.261$) among the four mean HYP concentrations.

4. Discussion

This study on the effect of HX-BGC on mineral contents of demineralized enamel and dentine provides information about the structure and morphology of the treated dental tissues. According to the results, HX-BGC and fluoride have a greater remineralizing effect on both demineralized enamel and dentine than that of deionized water, and the combined application of these two agents has a synergistic effect.

In the current study, an acidic solution was used to demineralize the tooth specimens for 8 days to create the lesions. The pH cycling model used was a chemical model described in a previous protocol paper [18] to mimic the oral situation for natural caries process. However, this is rather different from the real situation due to the absence of bacteria in the demineralization and remineralization processes. For specimen preparation, both prismatic and aprismatic enamel were used in previous caries studies. The reason we choose to cut prisms transversally is that lesion created in the surface of transversally-cut enamel are more reproducible than lesions created in the anatomical surface [21]. The temperature setting for pH cycling adopted in previous studies included both room temperature and 37℃ [22]. Application of the study agents twice per day simulates brushing teeth with a toothpaste in the morning and in the evening. For assessing collagen degradation, a modified hydroxyproline assay was applied in this study to measure the amount of degraded collagen in the dentine. Hydrochloric acid (HCl) is an inexpensive and easily available strong acid, and it can be a safer alternative to perchloric acid ($HClO_4$) used in hydroxyproline assay without affecting the amino acid measurement [20]. A previous study found that, in the fixation process, the minerals of dentine can be dissolved by the formic acid produced by formaldehyde [23]. In the present study, all specimens were fixed in 2.5% glutaraldehyde instead of formaldehyde for a night before being observed under the SEM, which stablized the collagen and preserved the minerals in the specimens.

Bioactive glass can remineralize dental hard tissues. The process involves release of ions (Ca^{2+}, PO_4^{3-}, etc.) from the bioactive glass network into the oral fluid and then the supersaturated ions in the fluid precipitate on the dental hard tissues [12, 24]. The essential conditions for remineralizing enamel and dentine include the followings. First, presence of mineral residues on the demineralized enamel and dentine to serve as apatite formation nuclei [25]. Second, abundant amount of calcium and phosphate ions in the surrounding environment of the remineralizing agent [26]. Third, intact dentine collagen to serve as a scaffold for mineral crystals to grow on [27]. The conditions in this study provided a favorable environment, which favored the precipitation of calcium phosphate and other ions, promoted apatite formation on the surface of demineralized enamel and dentine.

The SEM images in this study show the demineralized enamel had a porous surface with absence of mineral deposition. This finding is consistent with that of a previous study which showed a rough and porous morphology of the artificial enamel lesions [28]. Moreover, previous studies found the demineralized enamel surfaces were covered by irregular mineral depositions after remineralization with bioactive glass or modified bioactive glass [29, 30], which is consistent with the finding of this study.

Mineral regain can be measured using different indicators, such as protein/mineral composition [31] or mineral density and microhardness [32]. The micro-CT results in this study show the use of HX-BGC and fluoride induced mineral precipitation on the surface of the demineralized enamel and dentine. When the HX-BGC reacted with fluid, the pH of the suspension increased and deposition of calcium and phosphate occurred to form new apatite in the nucleation sites on the demineralized enamel and dentine surfaces [33].

According to our previous study on the effect of HX-BGC and fluoride on apatite crystallization, strontium can be incorporated into the crystal lattice of hydroxyapatite due to its chemical similarity to calcium [34, 35]. Strontium has an ionic radius larger than calcium (Ca^{2+}: 0.94Å, Sr^{2+}: 1.16Å) [36] which explains the lower 2θ value of the peak in the spectrum of Group 1 in this study. Moderate amount of strontium can up-regulate osteoblast activity that favors bone formation. Thus, attention should be paid to the incorporation of an optimal level of strontium into bioactive glass [34]. The shift to higher 2θ value in this study is likely due to fluoride ion, which has a radius smaller than hydroxyl ion [37]. Fluoride release from bioactive glass will increase in the presence of strontium [38]. Having strontium and fluoride incorporated into the apatite crystal lattice can enhance the bioactivity and chemical stability of the newly formed apatite [35].

An intact dentine collagen structure plays a key role in remineralization because it can serve as a nucleation center [27]. The organic matrix of dentine primarily consists of type I collagen, which has HYP as a major component and plays a key role in stabilizing the dentine collagen. A modified HYP assay was used in this study for direct evaluation of collagen after dentine degradation. Research suggests that MMPs in dentine or in saliva have an important effect on the degradation of dentine collagen [39]. MMPs are endogenous dentinal proteases (secreted as inactive zymogens) and the activation of these intrisinc proteases can induce breakdown of the proteins within the dentine matrix through hydrolysis and proteolysis [40],

resulting in a decrease of HYP [41]. Activation of MMP-2, MMP-8 and MMP-9 which can be initiated by a pH fall is the main reason for collagen degradation [3]. It should be noted that strontium can down-regulate the expression level of MMP-2 and MMP-9 and thus can inhibit the process of collagen degradation [15]. Moreover, strontium has been reported to increase the level of type I collagen [42] and promote synthesis of HYP [43], but it can stimulate the formation of collagen at specific concentrations (1 and 2.5mM) only [44]. In this study, the concentration of strontium from HX-BGC should be at a low level which cannot meet the requirement for inhibiting MMPs expression. Despite this, relatively intact collagen network was observed in all the groups except control under SEM.

The chemical model used in this study and the methods used for analysis have their limitations. First, biological factors should be added to the pH-cycling procedure to mimic the real situation in the oral cavity. Second, lack of XRD images after 8-day demineralization does not allow the comparison on apatite characteristics before and after pH cycling. Further experiments should include additional assessments, such as nuclear magnetic resonance (NMR) spectroscopy, to confirm the exact apatite types formed in remineralization process. Further laboratory studies should apply a proper biological model to investigate the remineralizing effect of HX-BGC and clinical trials should be conducted to provide evidence for supporting its clinical application.

5. Conclusion

The new strontium-doped bioactive glass (HX-BGC) can reduce mineral loss and promote remineralization of demineralized enamel and dentine through the precipitation of newly formed apatite. Moreover, strontium-doped bioactive glass and fluoride have a sygnergistic effect on demineralized dental hard tissues.

Funding

This study was supported by the Tam Wah-Ching Endowed Professorship of the University of Hong Kong.

Table 1. Mean lesion depths (μm) and mineral loss (g/cm^3) of the dentine and enamel in four groups

Groups	Dentine		Enamel	
	Lesion depth (μm)	Mineral loss (g/cm^3)	Lesion depth (μm)	Mineral loss (g/cm^3)
HX-BGC (1)	152.60 ± 5.18	1.64 ± 0.09	80.84 ± 2.43	3.15 ± 0.18
HX-BGC+F (2)	140.88 ± 12.82	1.54 ± 0.11	50.60 ± 10.65	2.94 ± 0.21
F (3)	165.36 ± 31.51	1.77 ± 0.08	72.67 ± 12.73	3.09 ± 0.23
Water (4)	214.12 ± 11.08	2.12 ± 0.08	130.66 ± 12.31	3.44 ± 0.07
p value	$p<0.001$	$p<0.001$	$p<0.001$	$p=0.005$
Multiple comparison	(1), (2), (3)<(4)	(1), (2)<(3)<(4)	(2)<(1), (3)<(4)	(2)<(4)

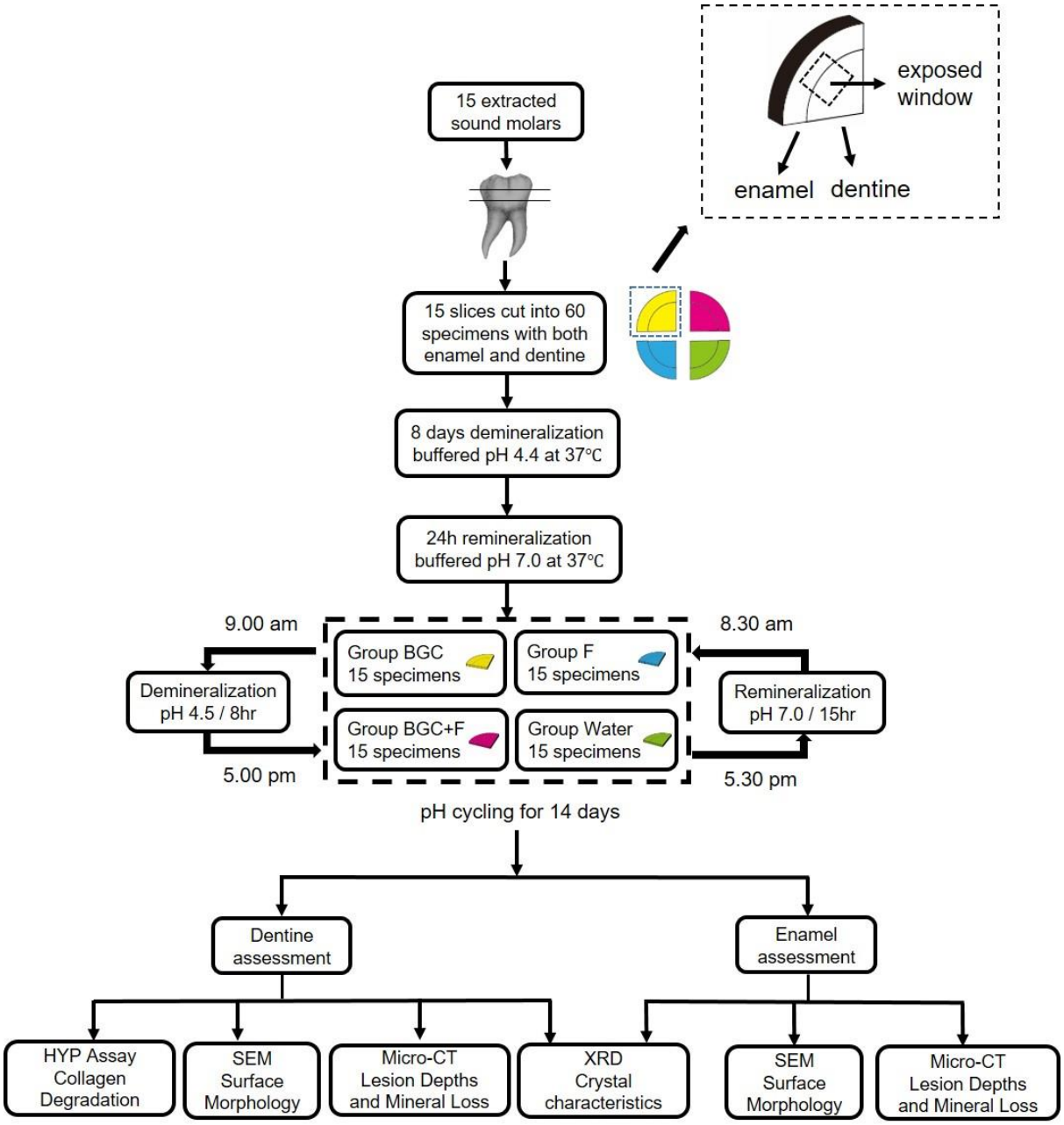

Figure 1. The flowchart of the experimental procedure

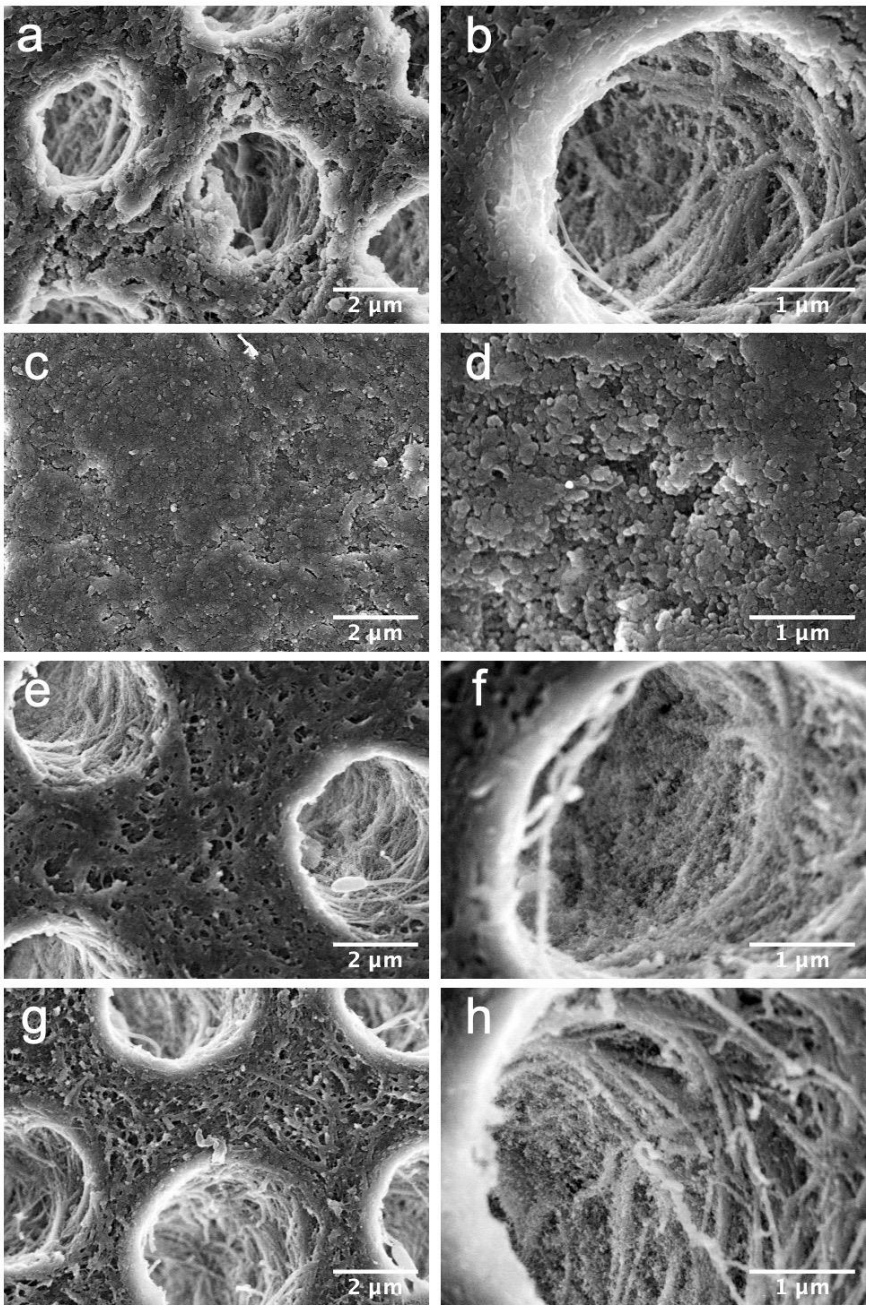

Figure 2. SEM images of the transverse surface of artificial dentine lesion. (a) 8000× magnification view of group HX-BGC showing granular particles in the inter-tubular area; (b) 20000× magnification view of group HX-BGC showing relatively intact collagen fibres; (c) 8000× magnification view of group HX-BGC + F showing no dentinal tubules exposure; (d) 20000× magnification view of group HX-BGC + F showing no exposure of dentine collagen; (e) 8000× magnification view of group F showing a relatively rough surface with partial exposure of collagen fibers; (f) 20000× magnification view of group F showing intact collagen fibres; (g) 8000× magnification view of group Water showing exposure of dentine collagen fibres in the inter- and intra-tubular areas; (h) 20000× magnification view of group Water showing loose intra-tubular collagen fibres.

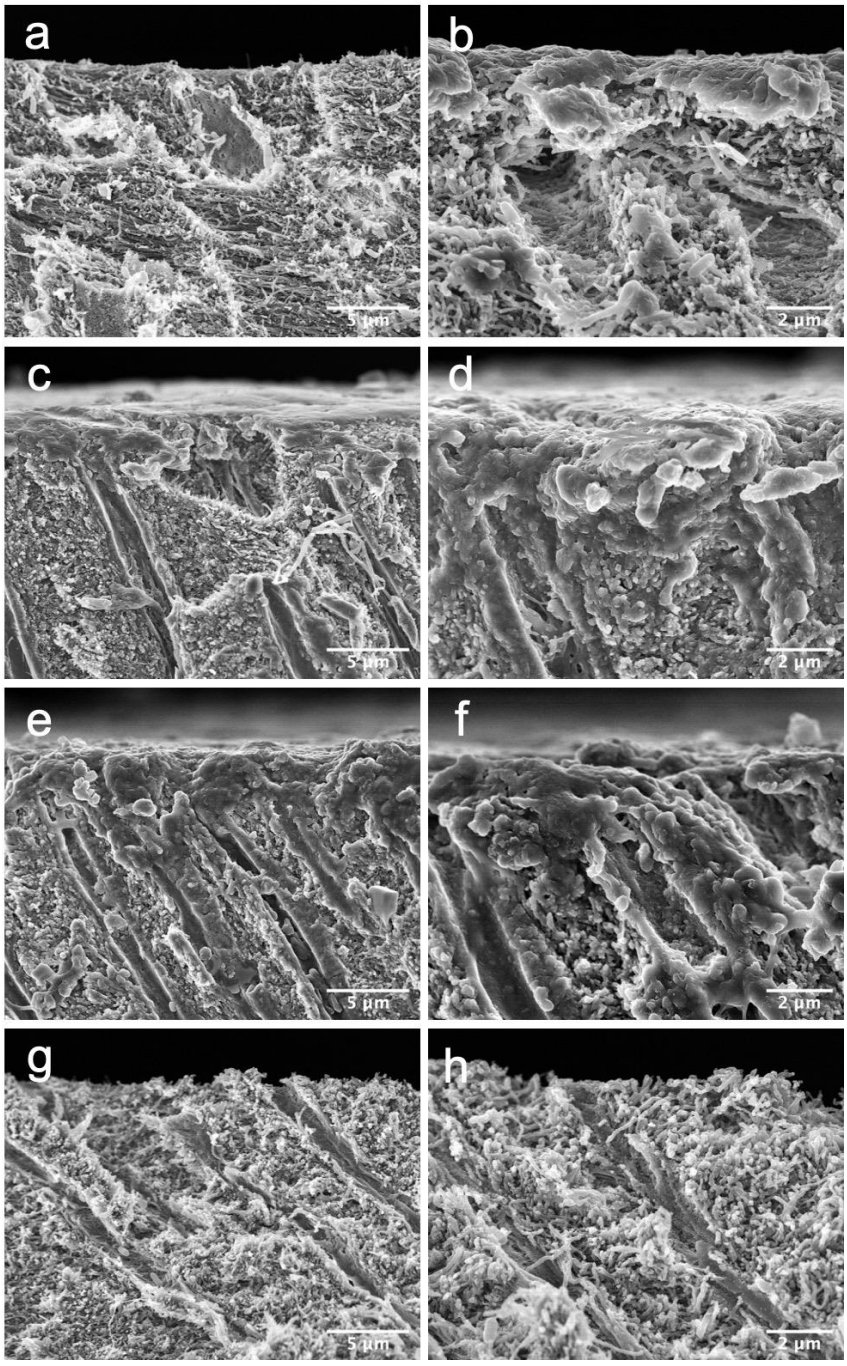

Figure 3. SEM images of the cross-sectional (longitudinal) surface of artificial dentine lesion. (a), (b) 4000× and 8000× magnification view of group HX-BGC showing granular structures on the surface; (c), (d) 4000× and 8000× magnification view of group HX-BGC + F showing large irregular particles on the cross-sectional surface and partially occluded dentine tubules; (e), (f) 4000× and 8000× magnification view of group F showing granular grains on the cross-sectional surface; (g), (h) 4000× and 8000× magnification view of group Water showing loose collagen fibres and no particles on the cross-sectional surface.

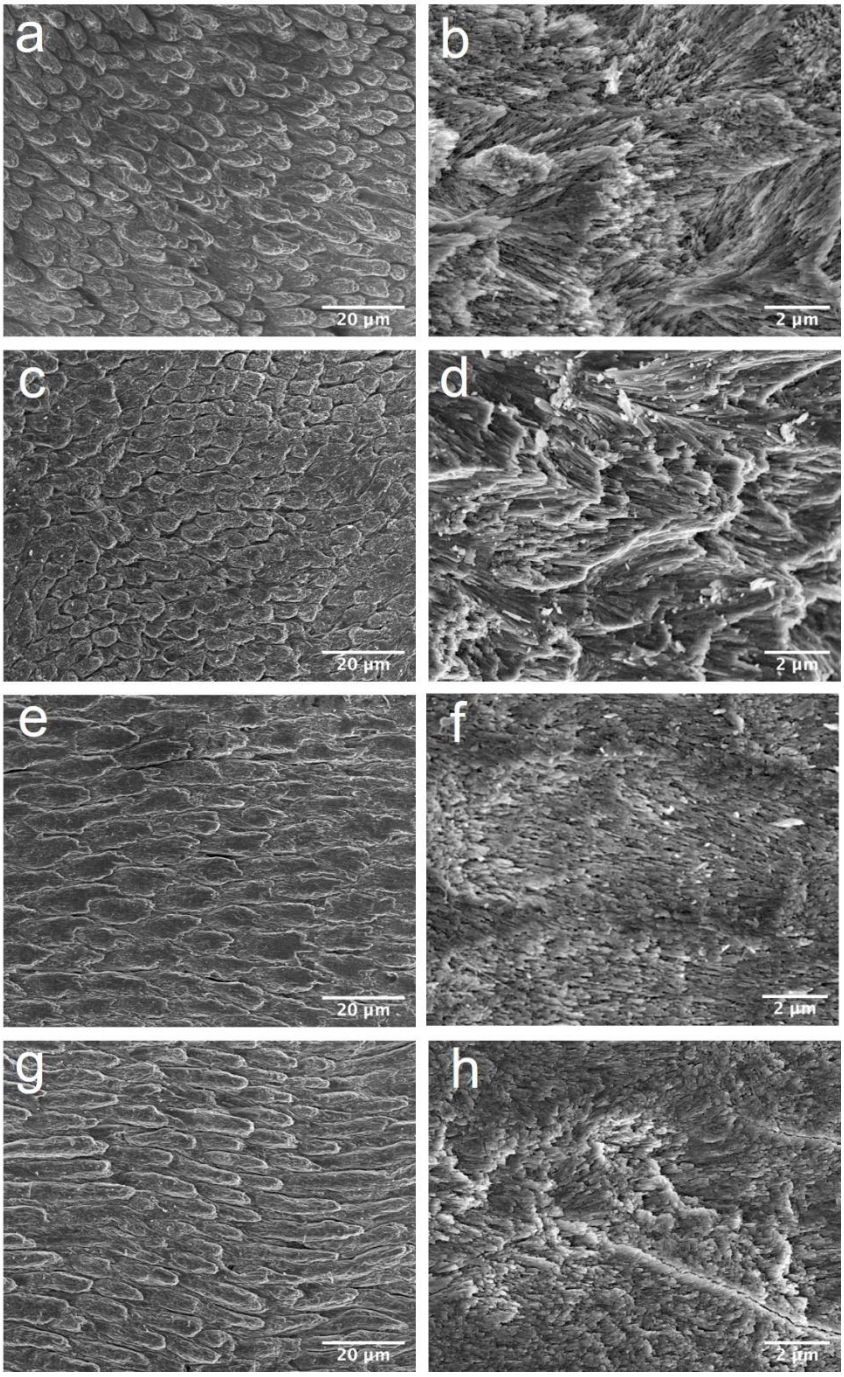

Figure 4. SEM images of the transverse surface of artificial enamel lesions. (a), (b) 1000× and 8000× magnification view of group HX-BGC showing regularly arranged enamel rods; (c), (d) 1000× and 8000× magnification view of group HX-BGC+ F showing tightly packed enamel rods; (e), (f) 1000× and 8000× magnification view of group F showing regularly packed enamel rods; (g), (h) 1000× and 8000× magnification view of group Water showing thinner enamel rods with obvious crevices.

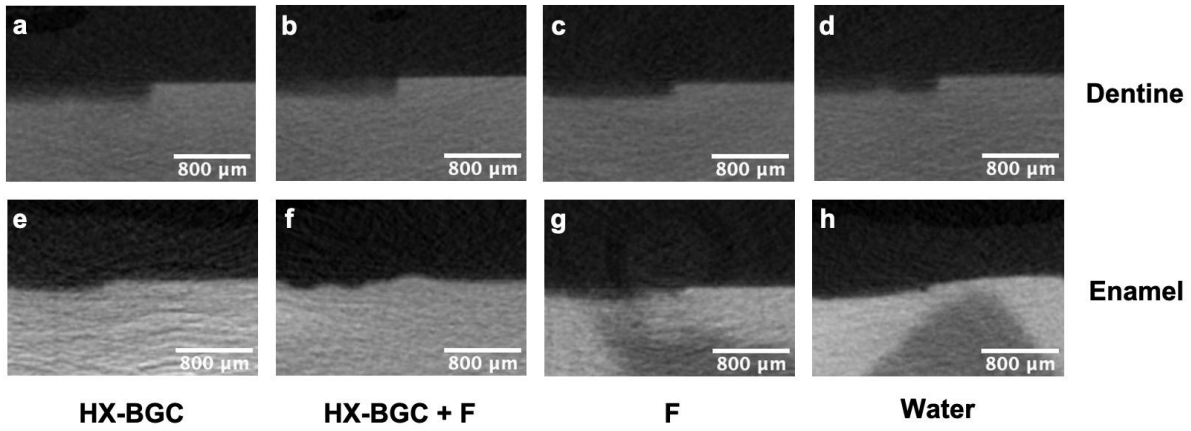

Figure 5. Micro-CT images of dentine and enamel lesions in the four groups after demineralization for 8 days

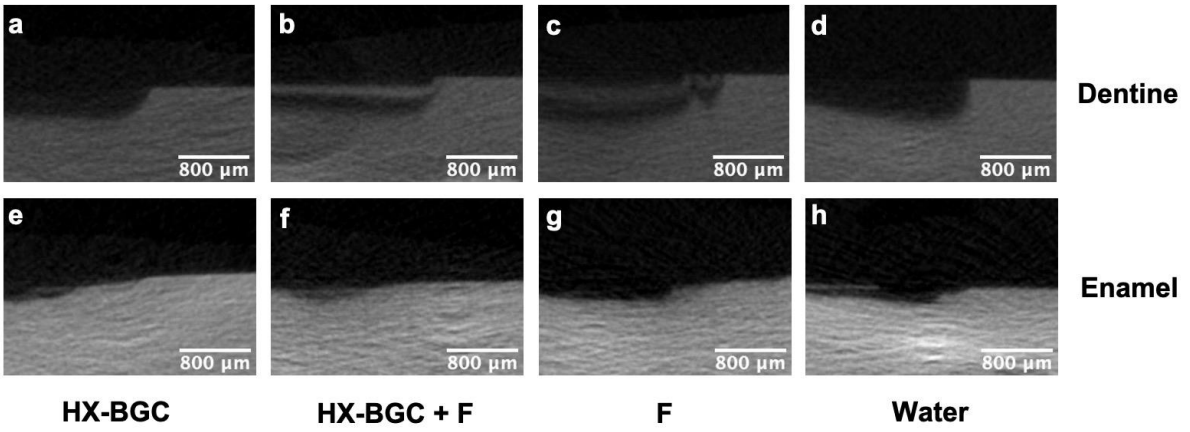

Figure 6. Micro-CT images of dentine and enamel lesions in the four groups after pH cycling and treatment.

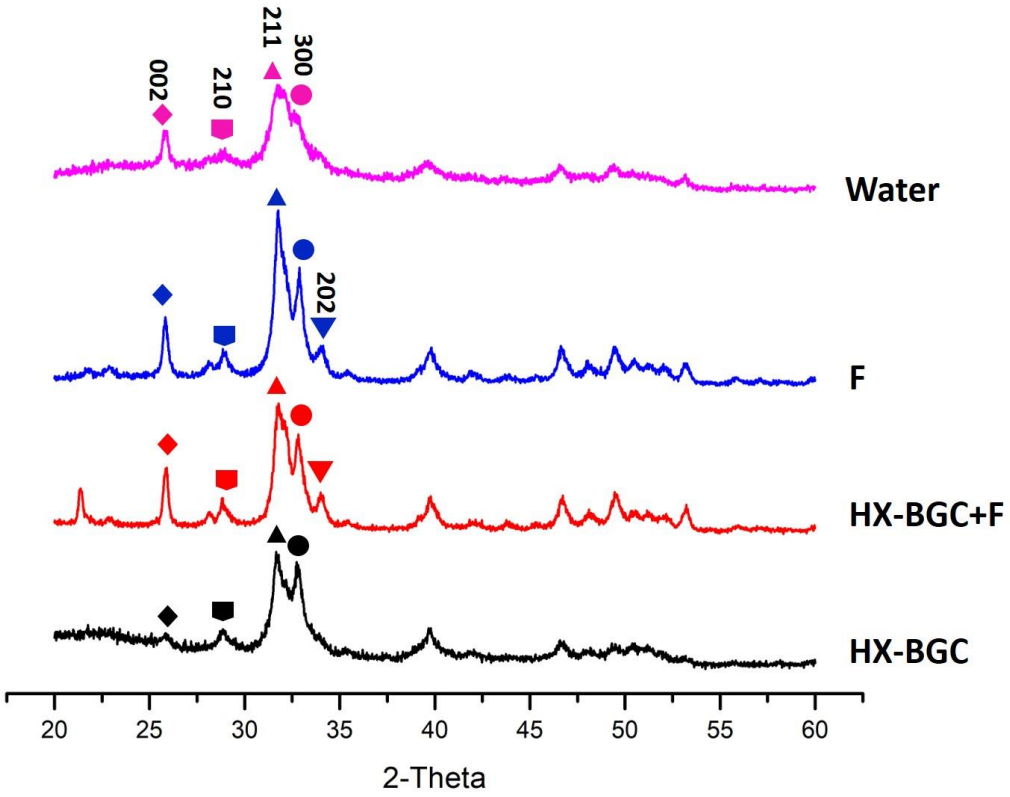

Figure 7. Typical XRD patterns of the four groups.

Reference

[1] J.D. Featherstone, Dental caries: a dynamic disease process, Australian dental journal 53(3) (2008) 286-91.

[2] R.H. Selwitz, A.I. Ismail, N.B. Pitts, Dental caries, Lancet (London, England) 369(9555) (2007) 51-9.

[3] M.L. Mei, Q.L. Li, C.H. Chu, C.K. Yiu, E.C. Lo, The inhibitory effects of silver diamine fluoride at different concentrations on matrix metalloproteinases, Dental materials : official publication of the Academy of Dental Materials 28(8) (2012) 903-8.

[4] N.B. Pitts, D.T. Zero, P.D. Marsh, K. Ekstrand, J.A. Weintraub, F. Ramos-Gomez, J. Tagami, S. Twetman, G. Tsakos, A. Ismail, Dental caries, Nature reviews. Disease primers 3 (2017) 17030.

[5] C.H. Chu, M.L. Mei, E.C.M. Lo, Use of fluorides in dental caries management, Gen Dent 58(1) (2010) 37.

[6] N.P.T. Innes, C.H. Chu, M. Fontana, E.C.M. Lo, W.M. Thomson, S. Uribe, M. Heiland, S. Jepsen, F. Schwendicke, A Century of Change towards Prevention and Minimal Intervention in Cariology, Journal of dental research 98(6) (2019) 611-617.

[7] A. Tezvergil-Mutluay, R. Seseogullari-Dirihan, V.P. Feitosa, G. Cama, D.S. Brauer, S. Sauro, Effects of Composites Containing Bioactive Glasses on Demineralized Dentin, Journal of dental research 96(9) (2017) 999-1005.

[8] S. Ali, I. Farooq, K. Iqbal, A review of the effect of various ions on the properties and the clinical applications of novel bioactive glasses in medicine and dentistry, The Saudi dental journal 26(1) (2014) 1-5.

[9] L.L. Hench, The story of Bioglass, Journal of materials science. Materials in medicine 17(11) (2006) 967-78.

[10] A.S. Bakry, Y. Tamura, M. Otsuki, S. Kasugai, K. Ohya, J. Tagami, Cytotoxicity of 45S5 bioglass paste used for dentine hypersensitivity treatment, Journal of dentistry 39(9) (2011) 599-603.

[11] S. Sauro, T.F. Watson, I. Thompson, Dentine desensitization induced by prophylactic and air-polishing procedures: an in vitro dentine permeability and confocal microscopy study, Journal of dentistry 38(5) (2010) 411-22.

[12] L.L. Dai, M.L. Mei, C.H. Chu, E.C.M. Lo, Mechanisms of Bioactive Glass on Caries Management: A Review, Materials (Basel) 12(24) (2019).

[13] R. Jayasree, T.S.S. Kumar, S. Mahalaxmi, S. Abburi, Y. Rubaiya, M. Doble, Dentin remineralizing ability and enhanced antibacterial activity of strontium and hydroxyl ion co-releasing radiopaque hydroxyapatite cement, Journal of materials science. Materials in medicine 28(6) (2017) 95.

[14] M.E. Curzon, The relation between caries prevalence and strontium concentrations in drinking water, plaque, and surface enamel, Journal of dental research 64(12) (1985) 1386-8.

[15] S.K. Tat, J.P. Pelletier, F. Mineau, J. Caron, J. Martel-Pelletier, Strontium ranelate inhibits key factors affecting bone remodeling in human osteoarthritic subchondral bone osteoblasts, Bone 49(3) (2011) 559-67.

[16] L.L. Dai, M.L. Mei, C.H. Chu, E.C.M. Lo, Antibacterial effect of a new bioactive glass on cariogenic bacteria, Archives of oral biology 117 (2020) 104833.

[17] G.H. Yassen, F. Lippert, G. Eckert, J. Eder, A.F. Zandona, The effect of strontium and combinations of strontium and fluoride on the remineralization of artificial caries lesions in vitro, Quintessence Int 43(7) (2012) e95-103.

[18] B.T. Amaechi, Protocols to Study Dental Caries In Vitro: pH Cycling Models, Methods Mol Biol 1922 (2019) 379-392.

[19] C.P. Kurtzman, F.L. Baker, M.J. Smiley, Specimen holder to critical-point dry microorganisms for scanning electron microscopy, Applied microbiology 28(4) (1974) 708-12.

[20] D.D. Cissell, J.M. Link, J.C. Hu, K.A. Athanasiou, A Modified Hydroxyproline Assay Based on Hydrochloric Acid in Ehrlich's Solution Accurately Measures Tissue Collagen Content, Tissue Eng Part C Methods 23(4) (2017) 243-250.

[21] J.M. ten Cate, P.P. Duijsters, Alternating demineralization and remineralization of artificial enamel lesions, Caries research 16(3) (1982) 201-10.

[22] M.A. Buzalaf, A.R. Hannas, A.C. Magalhães, D. Rios, H.M. Honório, A.C. Delbem, pH-cycling models for in vitro evaluation of the efficacy of fluoridated dentifrices for caries control: strengths and limitations, Journal of applied oral science : revista FOB 18(4) (2010) 316-34.

[23] M.L. Mei, L. Ito, Y. Cao, Q.L. Li, E.C. Lo, C.H. Chu, Inhibitory effect of silver diamine fluoride on dentine demineralisation and collagen degradation, J Dent 41(9) (2013) 809-17.

[24] D. Fernando, N. Attik, N. Pradelle-Plasse, P. Jackson, B. Grosgogeat, P. Colon, Bioactive glass for dentin remineralization: A systematic review, Materials science & engineering. C, Materials for biological applications 76 (2017) 1369-1377.

[25] F.R. Tay, D.H. Pashley, Guided tissue remineralisation of partially demineralised human dentine, Biomaterials 29(8) (2008) 1127-37.

[26] M.C. Peters, Strategies for noninvasive demineralized tissue repair, Dental clinics of North America 54(3) (2010) 507-25.

[27] Y. Kuboki, K. Ohgushi, T. Fusayama, Collagen biochemistry of the two layers of carious dentin, Journal of dental research 56(10) (1977) 1233-7.

[28] J. Zhang, V. Boyes, F. Festy, R.J.M. Lynch, T.F. Watson, A. Banerjee, In-vitro subsurface remineralisation of artificial enamel white spot lesions pre-treated with chitosan, Dental materials : official publication of the Academy of Dental Materials 34(8) (2018) 1154-1167.

[29] Y. Wang, L. Mei, L. Gong, J.L. Li, S.W. He, Y. Ji, W.B. Sun, Remineralization of early enamel caries lesions using different bioactive elements containing toothpastes: An in vitro study, Technol Health Care 24(5) (2016) 701-711.

[30] H. Milly, F. Festy, T.F. Watson, I. Thompson, A. Banerjee, Enamel white spot lesions can remineralise using bio-active glass and polyacrylic acid-modified bio-active glass powders, Journal of dentistry 42(2) (2014) 158-66.

[31] M. Vollenweider, T.J. Brunner, S. Knecht, R.N. Grass, M. Zehnder, T. Imfeld, W.J. Stark, Remineralization of human dentin using ultrafine bioactive glass particles, Acta biomaterialia 3(6) (2007) 936-43.

[32] F. Schwendicke, A. Al-Abdi, A. Pascual Moscardó, A. Ferrando Cascales, S. Sauro, Remineralization effects of conventional and experimental ion-releasing materials in chemically or bacterially-induced dentin caries lesions, Dental materials : official publication of the Academy of Dental Materials 35(5) (2019) 772-779.

[33] A.B. Mehta, V. Kumari, R. Jose, V. Izadikhah, Remineralization potential of bioactive glass and casein phosphopeptide-amorphous calcium phosphate on initial carious lesion: An in-vitro pH-cycling study, J Conserv Dent 17(1) (2014) 3-7.

[34] D. Sriranganathan, N. Kanwal, K.A. Hing, R.G. Hill, Strontium substituted bioactive glasses for tissue engineered scaffolds: the importance of octacalcium phosphate, Journal of materials science. Materials in medicine 27(2) (2016) 39.

[35] L.L. Dai, F. Nudelman, C.H. Chu, E.C.M. Lo, M.L. Mei, The effects of strontium-doped bioactive glass and fluoride on hydroxyapatite crystallization, Journal of dentistry (2021) 103581.

[36] C. Bussola Tovani, A. Gloter, T. Azais, M. Selmane, A.P. Ramos, N. Nassif, Formation of stable strontium-rich amorphous calcium phosphate: Possible effects on bone mineral, Acta biomaterialia 92 (2019) 315-324.

[37] M.L. Mei, F. Nudelman, B. Marzec, J.M. Walker, E.C.M. Lo, A.W. Walls, C.H. Chu, Formation of Fluorohydroxyapatite with Silver Diamine Fluoride, Journal of dental research 96(10) (2017) 1122-1128.

[38] H.O. Simila, N. Karpukhina, R.G. Hill, Bioactivity and fluoride release of strontium and fluoride modified Biodentine, Dental materials : official publication of the Academy of Dental Materials 34(1) (2018) e1-e7.

[39] D.H. Pashley, F.R. Tay, C. Yiu, M. Hashimoto, L. Breschi, R.M. Carvalho, S. Ito, Collagen degradation by host-derived enzymes during aging, Journal of dental research 83(3) (2004) 216-21.

[40] S. Sauro, D.H. Pashley, Strategies to stabilise dentine-bonded interfaces through remineralising operative approaches – State of The Art, International journal of adhesion and adhesives 69 (2016) 39-57.

[41] C. Chaussain-Miller, F. Fioretti, M. Goldberg, S. Menashi, The role of matrix metalloproteinases (MMPs) in human caries, Journal of dental research 85(1) (2006) 22-32.

[42] J. Liu, S.C. Rawlinson, R.G. Hill, F. Fortune, Strontium-substituted bioactive glasses in vitro osteogenic and antibacterial effects, Dental materials : official publication of the Academy of Dental Materials 32(3) (2016) 412-22.

[43] J. Wang, X. Zhu, L. Liu, X. Shi, L. Yin, Y. Zhang, X. Li, Z. Wang, G. Liu, Effects of strontium on collagen content and expression of related genes in rat chondrocytes cultured in vitro, Biological trace element research 153(1-3) (2013) 212-9.

[44] M. Huang, R.G. Hill, S.C. Rawlinson, Strontium (Sr) elicits odontogenic differentiation of human dental pulp stem cells (hDPSCs): A therapeutic role for Sr in dentine repair?, Acta biomaterialia 38 (2016) 201-11.